Flavonoid Accumulation Patterns of Transparent Testa Mutants of Arabidopsis[1]

Wendy Ann Peer,* Dana E. Brown, Brian W. Tague, Gloria K. Muday, Lincoln Taiz, and Angus S. Murphy

Department of Horticulture and Landscape Architecture, Purdue University, West Lafayette, Indiana 47907 (W.A.P., A.S.M.); Department of Biology, Wake Forest University, Winston-Salem, North Carolina 27109 (D.E.B., B.W.T., G.K.M.); and Biology Department, University of California, Santa Cruz, California 95064 (L.T.)

Flavonoids have been implicated in the regulation of auxin movements in Arabidopsis. To understand when and where flavonoids may be acting to control auxin movement, the flavonoid accumulation pattern was examined in young seedlings and mature tissues of wild-type Arabidopsis. Using a variety of biochemical and visualization techniques, flavonoid accumulation in mature plants was localized in cauline leaves, pollen, stigmata, and floral primordia, and in the stems of young, actively growing inflorescences. In young Landsberg *erecta* seedlings, aglycone flavonols accumulated developmentally in three regions, the cotyledonary node, the hypocotyl-root transition zone, and the root tip. Aglycone flavonols accumulated at the hypocotyl-root transition zone in a developmental and tissue-specific manner with kaempferol in the epidermis and quercetin in the cortex. Quercetin localized subcellularly in the nuclear region, plasma membrane, and endomembrane system, whereas kaempferol localized in the nuclear region and plasma membrane. The flavonoid accumulation pattern was also examined in transparent testa mutants blocked at different steps in the flavonoid biosynthesis pathway. The transparent testa mutants were shown to have precursor accumulation patterns similar to those of end product flavonoids in wild-type Landsberg *erecta*, suggesting that synthesis and end product accumulation occur in the same cells.

Flavonoids comprise a diverse group of phenolic compounds that serve a variety of ecological and physiological functions in plants (Stafford, 1990; Mathesius et al., 1998a; Debeaujon et al., 2000). A possible role for phenolics in the regulation of auxin retention was first proposed by Stenlid (1976) and Marigo and Boudet (1977). One group of flavonoids, the aglycone flavonols, has been shown to inhibit polar auxin transport, thereby promoting auxin retention. In zucchini hypocotyls, aglycone flavonols displace the auxin transport inhibitor 1-*N*-naphthylphthalamic acid (NPA) from specific binding sites on the plasma membrane (Jacobs and Rubery, 1988; Faulkner and Rubery, 1992; Bernasconi, 1996). Aglycone flavonoids were highly active, whereas glycosides were not, as was found to be the case in studies of flavonoid regulation of auxin retention in clover roots (Mathesius et al., 1998b).

Flavonoid-deficient mutants provide useful tools for studying the roles of flavonoids in normal growth and development. The transparent testa (*tt*) phenotype affecting seed coat color in Arabidopsis results from defects in various steps in the flavonoid biosynthesis pathway (Koornneef et al., 1982; Koornneef, 1990; Shirley et al., 1995; Fig. 1). As such, the *tt* mutants make it possible to analyze the effects of individual flavonoids on auxin transport and growth characteristics. The *tt4* alleles contain mutations in the gene encoding CHS and, as there is only a single gene encoding this enzyme in Arabidopsis, these plants are deficient in flavonoids (Saslowsky et al., 2000). In a recent series of studies, two *tt4* alleles were examined and were found to have altered auxin transport in seedlings and inflorescence tissue, as compared with wild-type seedlings (Murphy et al., 2000, Brown et al., 2001). In one of those studies (Murphy et al., 2000), treatment of seedlings with naringenin, a flavonoid precursor, restored flavonoid biosynthesis in the *tt4* mutant, resulting in the normal auxin distribution profile and loss of auxin efflux from the mutant root. Thus, there is mounting evidence that auxin retention or transport in vivo is regulated by the accumulation of aglycone flavonols.

Additional evidence in support of the hypothesis that flavonoids act to regulate auxin transport is that these compounds accumulate in tissues where auxin transport may be regulated. Murphy et al. (2000) recently demonstrated tissue-specific localization of flavonoids in Arabidopsis seedlings. Quercetin, kaempferol, and naringenin chalcone (NC) were shown to be concentrated in three tissues: the upper hypocotyl (UH), the hypocotyl-root transition zone

[1] This work was supported by the U.S. Department of Agriculture (grant no. 94–37100–0755 to L.T.), by Sigma Xi (grant to D.E.B.), and by the National Aeronautical and Space Administration (grant no. NAG2 1203 to G.K.M.). The Wake Forest University Research and Publications Fund and Purdue Agricultural Research Programs (manuscript ID no. 16464) supported the publication costs.

* Corresponding author; e-mail peer@hort.purdue.edu; fax 765–494–0391.

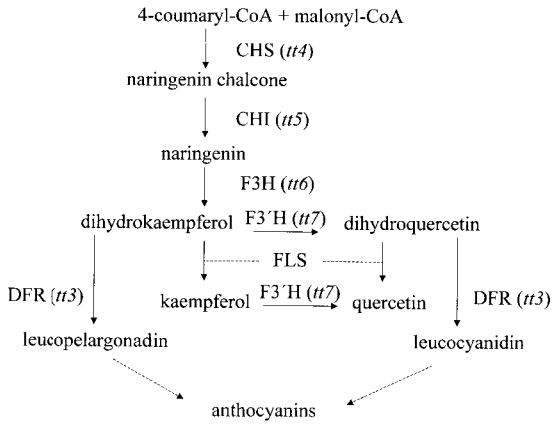

Figure 1. Schematic diagram of the flavonoid biosynthetic pathway. CHS, chalcone synthase; CHI, chalcone isomerase; F3H, flavanone 3-hydroxylase; F3′H, flavonoid 3′-hydroxylase; FLS, flavonol synthase; DFR, dihyroflavonol 4-reducatase. Specific *tt* mutations are indicated. Each enzyme product can potentially undergo glycosylation.

(TZ), and the distal elongation region of the root. These same tissues have been shown to be sites of auxin accumulation in Arabidopsis seedlings, as determined by direct measurement of radiolabeled indole-3-acetic acid transport (Murphy et al., 2000) and by the expression of auxin-responsive reporter genes (Ulmasov et al., 1997; Sabatini et al., 1999). Therefore, flavonoids appear appropriately distributed to regulate auxin movement.

It is probable that only specific flavonoid compounds are going to be active as regulators of auxin movement in plants. To determine which compounds are active, a number of mutants with lesions at different enzymes in the flavonoid biosynthetic pathway were examined. The *tt4* mutations in the chalcone synthase (*CHS*) gene are deficient in flavonoid accumulation, but accumulate an excess of sinapate esters (Saslowsky et al., 2000); the *tt5* lesion in the CHI gene, accumulates NC in place of flavonols, but has wild-type levels of sinapate esters; the *tt7* mutant in the flavonoid 3′-hydroxylase gene (F3′H) accumulates an excess amount of kaempferol; and a *tt3* lesion in the gene encoding DFR, accumulates excess amounts of quercetin and kaempferol, as predicted from the pathway and confirmed experimentally (Koornneef et al., 1982; Shirley et al., 1995; Graham, 1998).

In this paper flavonoid-deficient *tt* mutants have been used to determine if flavonols are transported from their site of synthesis to their site of accumulation. The flavonoid content in whole seedlings of Arabidopsis and the *tt* mutants was previously determined by Shirley et al. (1995) and Burbulis et al. (1996) using thin-layer chromatography (TLC), HPLC, and mass spectroscopy (MS), and by Sheahan (1996) and Sheahan and Cheong (1998) by HPLC and diode array analysis. These previous publications did not provide information on where these compounds were accumulating. In a previous study (Murphy et al., 2000), visualization of tissue-specific flavonoid accumulation was limited to 4-d whole wild-type seedlings with the intention of correlating flavonoid localization with regions of auxin accumulation. Here, the accumulation of flavonol precursors and their end products in specific tissue segments and subcellular regions were characterized in wild-type and *tt* mutant plants by a combination of histochemical fluorescence staining with diphenylboric acid-2-aminoethyl ester (DPBA), two-dimensional TLC, HPLC, fluorometry, UV/vis spectroscopy, and MS. The results from these analyses indicate that the location of flavonoid accumulation is unchanged when the later reactions of the pathway are inhibited.

In this report we have also expanded flavonoid localization studies in seedlings, extended the studies to include mature plants, and supplemented histochemical fluorescence assays with chemical analyses to confirm the identity of flavonoid intermediates. We have applied these studies to a range of *tt* mutants blocked at various stages in the flavonoid biosynthetic pathway to determine the localization of flavonoid intermediates.

RESULTS

Identification and Quantitation of Flavonoid Species in Wild-Type Arabidopsis Tissues

Flavonoids in wild-type and mutant seedlings were identified in three main zones: the cotyledonary node, the hypocotyl/root TZ, and the root tip. After dissection of seedlings, the endogenous flavonoids in the three zones were extracted and identified by two-dimensional TLC, HPLC, fluorometry, UV/vis spectroscopy, and MS by comparison with known standards (hereafter, for the sake of brevity, referred to as "spectral analysis"). Aglycones and substituted flavonoids were detected. For each region the major flavonoid skeletons identified as well as the specific genetic lesion found in each *tt* mutant are indicated in Table I. In all cases except *tt6*, the flavonoid intermediate expected to accumulate as a result of the specific biosynthetic defect was detected. Naringenin is the intermediate expected to accumulate in *tt6*; however, it was never detected in mutant or wild-type seedlings. In addition, the lesion in *tt6* is leaky, and therefore, end-product flavonoids were also detected.

To obtain more quantitative information on the flavonoid concentration in these tissue segments, the same three segments were excised and the aglycone flavonols were purified by HPLC and were quantified by UV/vis spectroscopy and mass spectrometry. The amounts of quercetin and kaempferol in the different regions are presented in Table II. In the wild type, the TZ/UR is the major site for accumulation of quercetin and kaempferol followed by the UH. Kaempferol accumulated in the LR, and a small

Table I. *Summary of tt mutations and major flavonoids accumulated and tissue-specific flavonoid localization in 5-d seedlings determined hystochemically and confirmed biochemically*

Line	Enzyme Mutated[a]	Flavonoid Accumulated[a]	Cotyledonary Node	TZ	Root Tip
tt4 (85)	CHS (null phenotype)	n.d.[b]	n.d.	n.d.	n.d.
tt5 (86)	CHI (null)	NC[c]	NC	NC	NC
tt6 (87)	F3H (leaky)	Narigenin[d]	NC, kaempferol, quercetin	NC, kaempferol, quercetin	NC, kaempferol
tt7 (88)	F3′H (null phenotype)	Kaempferol	Kaempferol	Kaempferol	NC, kaempferol
tt3 (84)	DFR (null)	Excess quercetin, Kaempferol	Quercetin, kaempferol	Quercetin, kaempferol	NC, quercetin, kaempferol

[a] Adapted from Koornneef et al. (1982); Shirley et al. (1995); and Wisman et al. (1998). [b] n.d., None detected. [c] NC, Naringenin chalcone. [d] Unidentified orthodihydroxy or orthotrihydroxy flavonoid accumulated (Sheahan et al., 1998).

amount of quercetin was found in the LH (Table II). High SDs found in the normalized root tip concentrations shown reflects the difficulty in obtaining accurate weights of those tissues.

In HPLC analyses of seedling sections, it was possible to determine the relative abundance of aglycone flavonols. In Table III, the proportion of total flavonoids that are aglycone flavonols is reported as a function of age and region of the seedling. The cotyledon contained mainly glycosylated flavonoids, with the amounts of aglycone flavonols decreasing as the tissue matured (Table III). In the UH, aglycone flavonols were the predominant flavonoids at 3 d, decreasing over time (Table III). In the LH, aglycone flavonols peaked at 5 d and decreased to one-third the total amount of flavonoids at 7 d (Table III). The same pattern was observed in the TZ/UR, with aglycone flavonols predominating at 5 d and glycosylated flavonoids comprising the majority at 7 d (Table III). In the LR, aglycone flavonols appeared to be the principal form at every time point (Table III).

Quantitation of Flavonoid Species in Tissues of *tt* Mutants of Arabidopsis

To determine how flavonoid distribution was affected by alterations in the enzymes in the flavonoid biosynthetic pathway, flavonoids were quantified in the *tt* mutants. Flavonoids were not detected in any section of *tt4* seedlings (Table II), as expected by the mutation in the *CHS* gene, which encodes an enzyme early in the flavonoid pathway. The *tt3* seedlings have a mutation in the gene encoding DFR, which is late in the flavonoid biosynthetic pathway, so flavonols such as quercetin and kaempferol would be expected to accumulate. In *tt3* seedlings, the TZ/UR was the primary site of quercetin and kaempferol accumulation. Compared with Landsberg *erecta* (Ler) seedlings, *tt3* contained significantly more quercetin in the UH, LH, and TZ/UR, and *tt3* also contained more kaempferol in the LH than wild-type seedlings (Table II). Whereas kaempferol alone was detected in Ler in the LR, kaempferol and quercetin accumulated in *tt3* (Table II).

Flavonols were not detected in *tt5* (Table II), and a peak consistent with NC, the intermediate expected to accumulate in this mutant, was detected. However, a peak containing a chalcone and flavanone skeleton with approximately the same retention time as quercetin and at a concentration of 5.3 ± 0.4 ng mg fresh weight^{-1} was observed in the UH in *tt5*. As NC does not have this retention time, spontaneous isomerization of NC to naringenin may have resulted in the subsequent formation of a flavanone structure in *tt5*.

The *tt7* mutant accumulated significantly more kaempferol in the UH and TZ/UR than did Ler (Table II), which is expected based on the mutation in the gene encoding F3′H. Within the kaempferol peaks, a minor chalcone skeleton (<1%) was detected spectroscopically. Like *tt5*, *tt7* also had peaks with approximately the same retention time as quercetin: 7-methyl-chalcone accumulated in the UH (63.3 ± 3.3 ng mg fresh weight^{-1}) and to a much lesser extent in the LH (5.3 ± 0.7 ng mg fresh weight^{-1}). A similar peak in the TZ/UR region was insufficient for definitive spectroscopic analysis. The accumulation of these other flavonoid compounds is not expected, as this mutant would not be predicted to exhibit altered conversion from flavanones and fla-

Table II. *HPLC determination of mean flavonol composition ± SD of 5-d-old Arabidopsis seedlings divided into sections*

Results were confirmed with fluorimetry, UV/vis spectroscopy, and mass spectroscopy. LH, Lower hypocotyl; TZ, transition zone; UR, upper root; LR, lower root. Means ± SD, $n = 3$. Asterisk indicates $P < 0.001$ compared with Ler by Student-Neumann-Keuls post hoc.

	Quercetin				Kaempferol			
Line	UH	LH	TZ/UR	LR	UH	LH	TZ/UR	LR
	ng/mg fresh wt				*ng/mg fresh wt*			
Ler	26.5 ± 4.2	5.3 ± 0.3	111 ± 7.9	0 ± 0.0	42 ± 3.4	0 ± 0.0	174 ± 10.3	84.8 ± 37.3
tt3	137 ± 6.2*	15 ± 0.8*	275 ± 12*	10.6 ± 7.22	42 ± 4.2	1.1 ± 0.4*	185 ± 16.3	127 ± 39.8
tt4	0 ± 0.0*	0 ± 0.0*	0 ± 0.0*	0 ± 0.0	0 ± 0.0*	0 ± 0.0	0 ± 0.0*	0 ± 0.0
tt5	0 ± 0.0*	0 ± 0.0*	0 ± 0.0*	0 ± 0.0	0 ± 0.0*	0 ± 0.0	0 ± 0.0*	0 ± 0.0
tt7	0 ± 0.0*	0 ± 0.0	0 ± 0.0*	0 ± 0.0	63 ± 4.4*	0 ± 0.0	296 ± 14.7*	111 ± 32.6

Table III. *Average ratio of aglycone flavonols ± SD to total flavonoids in 3-, 5-, and 7-d-old wild-type seedling sections by HPLC, fluorimetry, UV/vis spectroscopy, and mass spectroscopy (see "Materials and Methods")*

They were calculated by dividing the nanograms per milligram of aglycone fresh wt flavonols by the nanograms per milligram fresh wt of the total flavonoids.

d	Percent of Aglycone Flavonols				
	Cotyledon	UH	LH	TZ/UR	LR
3	22 ± 10	79 ± 14	78 ± 16	86 ± 15	106 ± 32
5	19 ± 7.9	14 ± 10	96 ± 16	96 ± 5.2	103 ± 20
7	14 ± 11	10 ± 9.9	36 ± 25	35 ± 15	87 ± 27

vonols. The accumulated flavonoids may be the result of altered feedback mechanisms in the mutants, and the compounds' subsequent availability to other enzymes. In the LR, kaempferol was also detected in *tt7* as in Ler. The presence of kaempferol in the LR seems to prevent leakage of auxin from the root tip (Murphy et al., 2000).

Time-Course of Flavonoid Staining

The results described above indicate that the concentrations of flavonoid intermediates change between wild-type and mutant plants. To examine the distribution of flavonoids in intact seedlings, a DPBA fluorescence time-course study showing the flavonoid accumulation patterns at different stages of development was performed, first in wild-type Ler and later with mutants. Each flavonoid-DPBA conjugate has a unique fluorescent color and a different intensity (e.g. quercetin fluorescence is 8× brighter than kaempferol when measured fluorometrically; data not shown). Table IV is a color key to the compounds described in this study as viewed through an FITC filter. Chlorophyll autofluorescence is red and sinapate ester autofluorescence is green. In Figure 2, autofluorescence of the cotyledonary node (Fig. 2A, inset) and the root/hypocotyls TZ (Fig. 2D, inset) are shown; root tips lacked sufficient autofluorescence to photograph. In Figure 2, the DPBA staining in seedlings at 3, 5, and 7 d after germination is shown. In the cotyledonary node, brilliant gold fluorescence corresponding to quercetin was detectable at 3 d (Fig. 2A) with the gold fluorescence increasing at 5 d (Fig. 2B) and quercetin and quercitrin (yellow-orange) observed at 7 d (Fig. 2C). In the TZ/UR, a small amount of quercetin and kaempferol (yellow-green) fluorescence was observed at 3 d (Fig. 2D). At 5 d, yellow-green fluorescence corresponding to kaempferol was in a single ring of cells (Fig. 2E, arrow) and a cone of quercetin-containing cells occurred in the root cortex beneath the kaempferol-containing ring (Fig. 2E). At 6 d, gold and yellow-orange fluorescence due to quercetin and quercitrin extended from the TZ throughout the length of the root (data not shown) and were found in the TZ at 7 d (Fig. 2F). Yellow fluorescence corresponding to NC was observed in the distal elongation zone at 3, 5, and 7 d (Fig. 2, G–I), whereas kaempferol (yellow-green) was found in the root cap at 5 d (Fig. 2H) and diminished at 7 d (Fig. 2I). The non-staining area between the root cap and the distal elongation zone is the meristematic region. The flavonoid staining patterns in each region were observed in >99% of the 500 seedlings that were examined.

Flavonoid localization in mature plants is presented in Figure 3. Sinapate ester fluorescence in whole plants appeared blue because they were visualized without a filter; the sinapate esters appeared green when viewed through an FITC filter. In wild-type adult plants that were actively growing (Fig. 3A), flavonoids were present in maturing siliques, inflorescence stems, cauline and rosette leaves, floral primordia, stigmata, and pollen (Fig. 3A, inset). In contrast, only blue sinapate ester autofluorescence was visible in unstained plants (Fig. 3B). However, in older mature plants that no longer had elongating inflorescence stems, the flavonoid staining was restricted to the actively growing tissues: the flowers, immature siliques, and upper inflorescence stems (Fig. 3C). In Ler, the principal flavonoid observed in the flowers and upper inflorescences was quercetin (gold), and the stigma papillae and pollen were also rich in quercetin (Fig. 3C, inset). The higher concentration of quercetin in these tissues was verified by spectral analysis. This flavonoid staining pattern occurred in all plants that were examined. In HPLC analyses of wild-type inflorescence stem segments, aglycone flavonoids were concentrated in the growing tissues and at the apex, and decreased toward the base, as shown in Figure 4. Flavonoids at the base were in the form of aglycones, glycosylated deriva-

Table IV. *Key to the fluorescent compound-DPBA conjugates described in this study*

Emission peak using fluorescein isothiocyanate (FITC) filter set.

Compound/Structure	Color	Emission Maxima
		nm
Sinapate esters/cell wall[a]	Green	515–516
Kaempferol	Yellow-green	520
NC	Yellow	527
Quercitrin	Yellow-orange	534
Quercetin	Gold	543
Chlorophyll/chloroplast[a]	Red	665–685

[a] Autofluorescence.

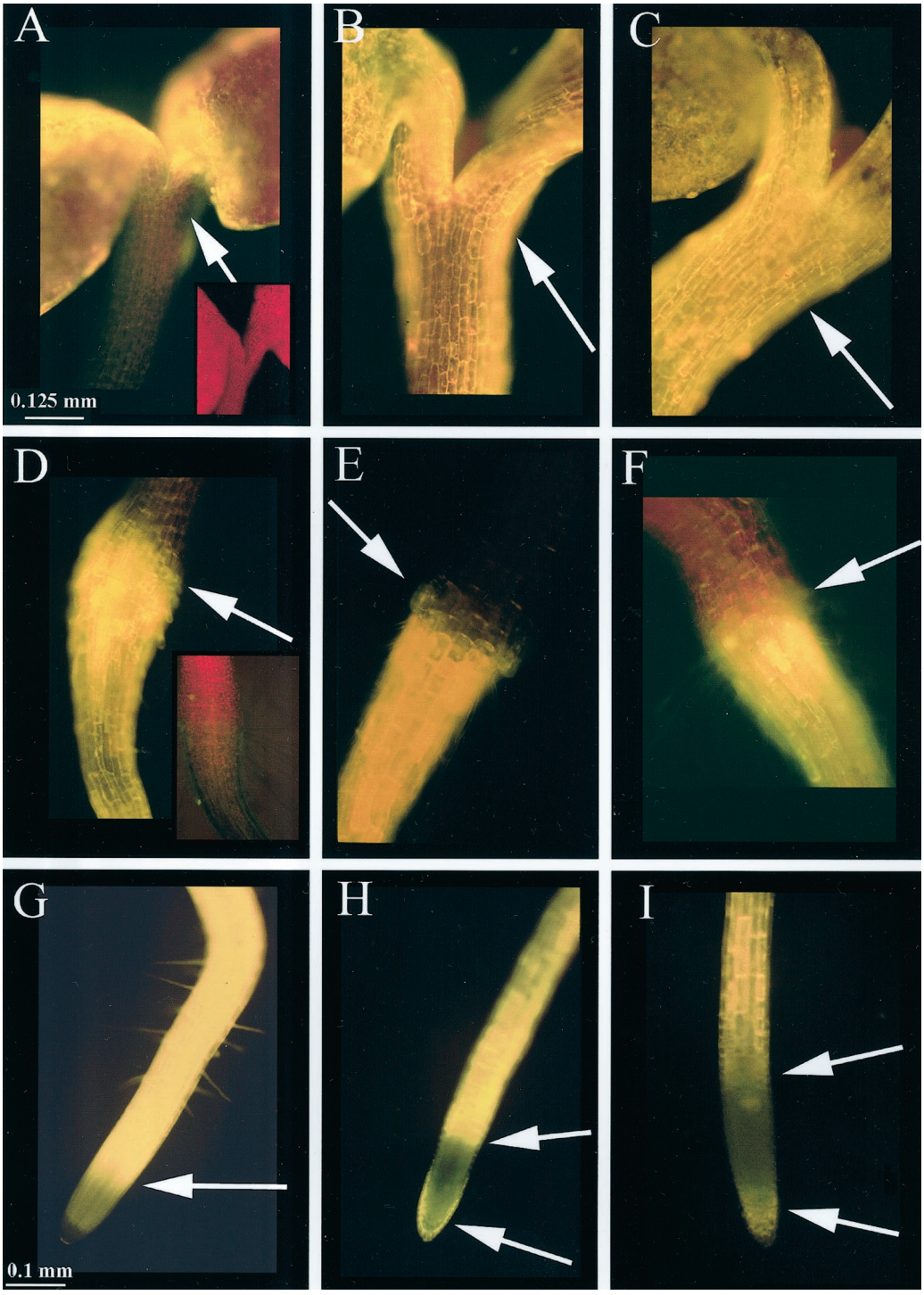

Figure 2. Time course of flavonoid accumulation in stained Ler seedlings viewed through an FITC filter. Size bars are 0.125 mm for A, B, C, D, E, and F and are 0.100 mm for G, H, and I. A through C, Cotyledonary nodes of 3-, 5-, and 7-d seedlings, respectively. The amount of quercetin (gold fluorescence) accumulation increases over time, and at 7 d quercitrin (glycosylated quercetin, yellow-orange fluorescence) is observed. Arrows point to cotyledonary nodes. A (inset), Autofluorescence of 3-d cotyledonary node; red color is due to chlorophyll. D through F, Hypocotyl/root TZ of 3-, 5-, and 7-d seedlings, respectively. The amounts of quercetin and kaempferol (yellow-green fluorescence) reach a maxima at 5 d, with kaempferol occurring in a ring of cells above the cone-shaped region of quercetin containing cells. Arrows point to transition zones. D (inset), Autofluorescence of 3-d TZ; red autofluorescence is due to chlorophyll and pale green autofluorescence is due to sinapate esters. G through I, Root tips of 3-, 5-, and 7-d seedlings, respectively. NC (yellow fluorescence) is observed in the distal elongation zone and kaempferol in the root cap. Arrows point to distal elongation zone (G–I) and root cap (H and I). The non-staining area is the meristematic region. Root tips lacked sufficient autofluorescence to photograph.

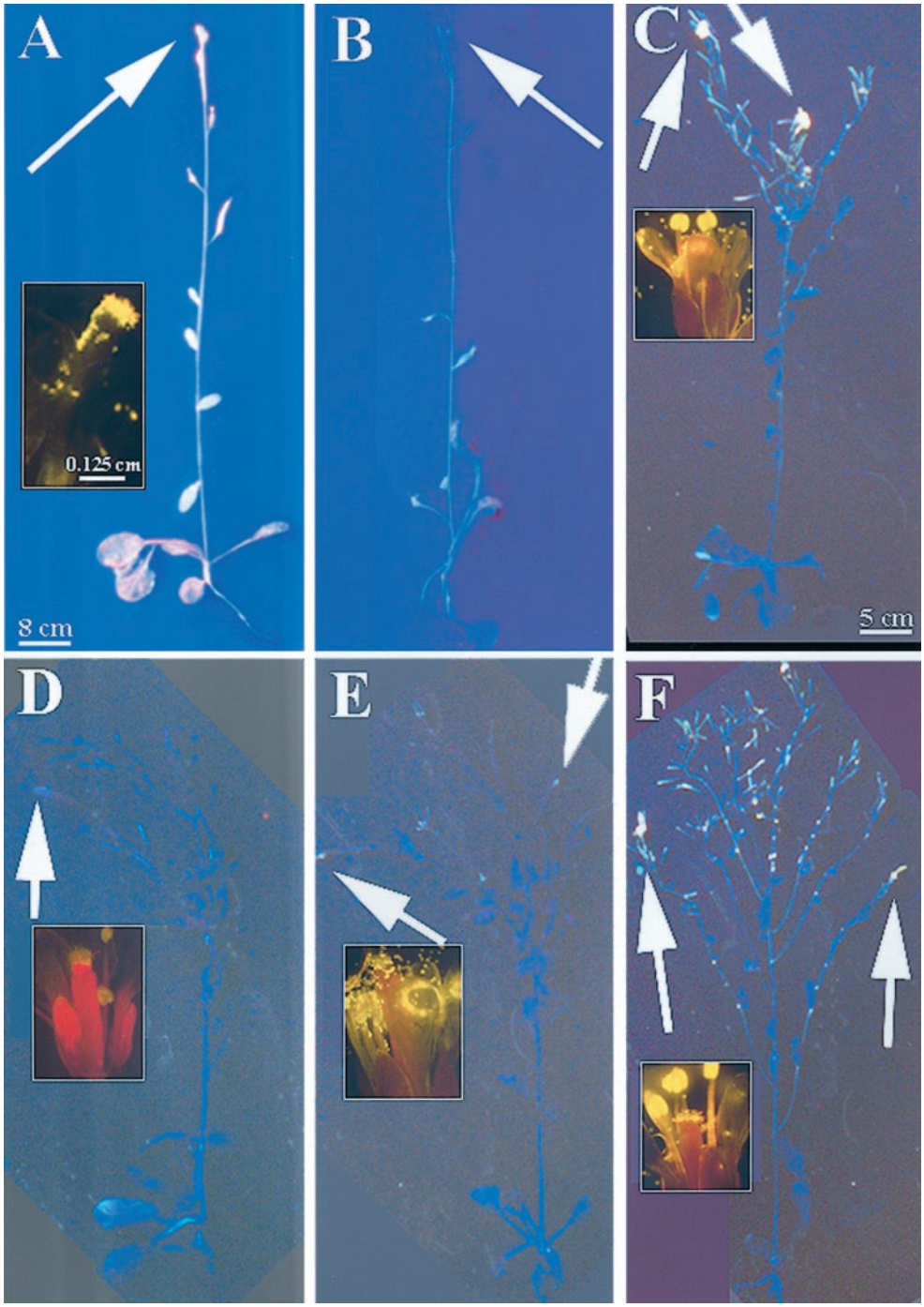

Figure 3. Flavonoid localization in inflorescences of wild-type and *tt* mutants. Arrows point to flowers. Size bar is 8 cm for whole plants in A and B, 5 cm for whole plants in D through F, and 0.125 mm for flower insets. A, Stained Columbia-0 (Col-0) with elongating inflorescence. Inset, Flower viewed through FITC filter. B, Autofluorescence Col-0 with elongating inflorescence. Sinapate ester autofluorescence is blue when viewed without a FITC filter. C, Stained Ler with nonelongating inflorescence. Inset, Flower viewed through FITC filter. D, Stained *tt4(85)* with nonelongating inflorescence. Inset, Flower viewed through FITC filter. E, Stained *tt5* with nonelongating inflorescence. Inset, Flower viewed through FITC filter. F, Stained *tt3* with nonelongating inflorescence. Inset, Flower viewed through FITC filter.

tives, and anthocyanin intermediates (Fig. 4). In segments containing cauline leaves (indicated by asterisks), the leaves and petioles were removed from the stem prior to HPLC analysis, and such cauline leaf nodes contained increased amounts of aglycone flavonoids (Fig. 4). Anthocyanins were most concentrated at the base of the stem, and decreased in concentration toward the apex (Fig. 4).

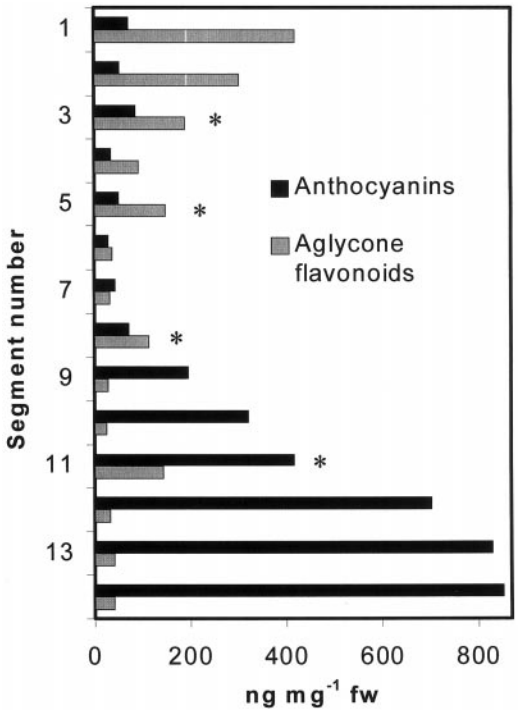

Figure 4. Anthocyanin and aglycone flavonoid content of inflorescence segments of Ler. Segment 1 corresponds to the <3-mm segment below floral cluster. Asterisk, Segment contained cauline leaf, which was excised prior to quantitation.

Flavonoid Staining in *tt* Mutants

Flavonoids accumulated in the same regions in the *tt* mutants as in wild-type seedlings. An unstained TZ of a *tt3* seedling showing background autofluorescence is presented in Figure 5A. Autofluorescence was encountered in all of the seedlings as a result of the presence of chlorophyll (red fluorescence) and sinapate esters (faint green fluorescence) in the epidermis and cell walls; *fah1-2* seedlings were used as a control for sinapate ester autofluorescence. In stained *tt4(85)* seedlings, only autofluorescence of the chlorophyll and sinapate esters was observed (Fig. 5B). In addition, *tt4(85)* had the same staining phenotype as the true null *tt4* (UV118a; data not shown). In all of the *tt* mutants, chloroplasts were observed in the upper one-third of the root. In *tt5* (Fig. 5C), NC (yellow) was observed in the TZ, and in *tt6* (Fig. 5D), a mixture of chalcone derivatives and end-product flavonoids were observed. In *tt7* (Fig. 5E), kaempferol (yellow-green) occurred in the same tissues that accumulated quercetin in the wild type. In *tt3* (Fig. 5F), the staining pattern was similar to that of wild type (Fig. 2E), except that kaempferol and quercetin (gold) accumulated in greater amounts than in wild type, as compared with Figure 2E, and as quantified in Table II. The pattern of flavonoid precursor and intermediate accumulation in the cotyledonary nodes and root tips was consistent with that of the flavonoids in the TZ (data not shown). These flavonoid staining patterns were observed in >98% of the 500 seedlings that were examined.

In mature *tt* plants, flavonoids also accumulated in growing tissues. In *tt4*, only sinapate ester florescence (blue fluorescence, no filter) was observed (Fig. 3D), and the pollen exhibited sinapate ester staining (faint green fluorescence, FITC filter; Fig. 3D, inset). In examination of *tt5* in Figure 3E, accumulation of NC (yellow) was detected in the floral primordia, stigmata, siliques, and pollen (Fig. 3E). This yellow fluorescence is much more obvious when the flowers are shown in the inset of Figure 3E, and was verified by spectral analysis. In *tt3*, the flavonoid staining pattern was similar to that observed in Ler, with quercetin accumulating in the upper inflorescences, floral primordia, stigmata, pollen, and siliques (Fig. 3F, inset), and verified by spectral analysis. These flavonoid staining patterns occurred in all observed plants.

Flavonoid Staining during Root Development

Flavonoid fluorescence was localized in the secondary root primordium as it protruded from the epidermis, as shown in a *tt3* root in Figure 6A. Flavonoid fluorescence was also visible at the base of the primordium at a later stage, in a representative *tt3* seedling (Fig. 6B). At the end of 7 d, when aglycone flavonoids were no longer detectable in the TZ or primary root, quercetin was found throughout the length of the secondary root, as shown in a wild-type seedling (Fig. 6C). In *tt4*, flavonoids were absent at the site of secondary root formation (Fig. 6D). During early secondary root development, the root primordium accumulated small amounts of flavonoids (Fig. 6E), as shown in a representative *tt7* plant. By 7 to 8 d, secondary roots had developed, and their flavonoid accumulation pattern was the same as that of the primary root, with fluorescence in the distal elongation zone and in the root cap (Fig. 6F), as shown in a wild-type seedling. These developmental and flavonoid staining patterns were observed in >98% of the seedlings.

Subcellular Staining of Flavonoids

To determine the subcellular distribution of flavonoid staining, the DPBA fluorescence in the roots of *tt3*, a mutant that accumulates excess flavonols, was examined under conditions that lead to mild plasmolysis, as in Figure 7A, or complete plasmolysis, as in Figure 7B. Under mild plasmolysis conditions, quercetin (gold) fluorescence was localized in the plasma membrane at the basal ends of root cells, as well as in the nuclear region (Fig. 7A). Under more stringent plasmolysis conditions, fluorescence was observed in the nuclear region, plasma membrane, and endomembrane system (Fig. 7B). In *tt7*, which only accumulates kaempferol (as shown in Table II),

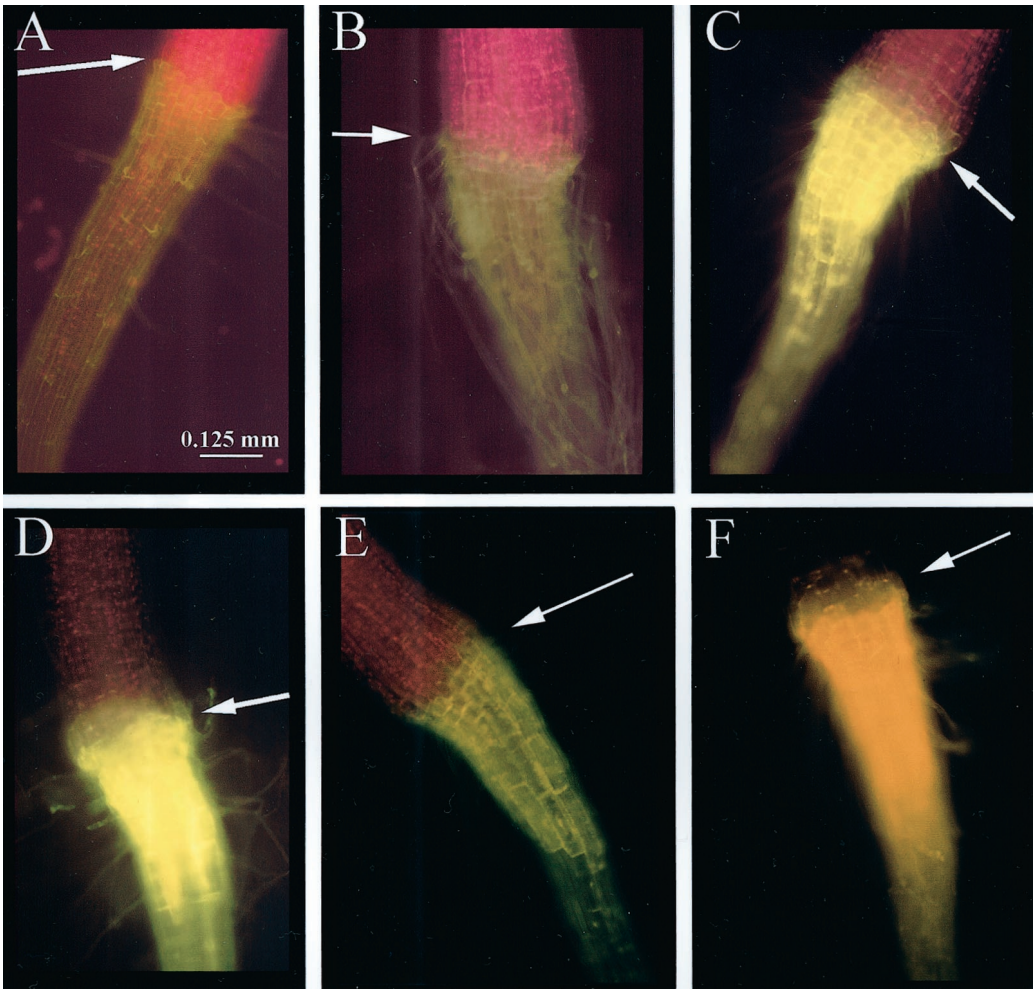

Figure 5. Flavonoid accumulation in the hypocotyl/root TZ in 5-d *tt* seedlings viewed through FITC filter. Arrows point to TZ. Size bar is 0.125 mm for A through F. A, Autofluorescence of *tt3* seedling. Chlorophyll autofluorescence red and sinapate esters a faint green. B, Stained *tt4(85)* seedling, which does not synthesize flavonoids and accumulates an excess of sinapate esters, only has autofluorescence of chlorophyll and sinapate esters. C, Stained *tt5* seedling accumulates NC (yellow fluorescence). D, Stained *tt6* seedling, a leaky mutation where NC is observed and small amounts of quercetin and kaempferol are present. E, Stained *tt7* seedling accumulates kaempferol (yellow-green fluorescence) in the ring zone and cone zone. F, Stained *tt3* seedling with saturated fluorescence of kaempferol and quercetin (gold fluorescence).

the yellow-green fluorescence of the DPBA-kampferol complex was localized in the nuclear region under mild plasmolysis conditions, as shown in Figure 7C. In *tt5*, which accumulates NC (as shown in Table I), fluorescence is observed throughout the cytosol (Fig. 7D). This pattern was observed in >90% of the seedlings observed.

DISCUSSION

Although the ability of aglycone flavonoids to inhibit auxin efflux and plasma membrane binding of the transport inhibitor NPA has been established for some time (Jacobs and Rubery, 1988; Bernasconi, 1996), evidence supporting a role for endogenous flavonoids in auxin transport has only recently been demonstrated (Murphy et al., 2000; Brown et al., 2001). Here we present evidence that flavonoids colocalize spatially and temporally with regions of auxin accumulation. Localization of aglycone flavonoids in areas of organ transition and maturation suggests that flavonoids may influence developmental processes through controlling the distribution of auxin in these tissues.

Flavonoid Accumulation

Flavonoid accumulation in seedlings is developmentally regulated and parallels the expression of the early genes of flavonoid biosynthesis, CHS, CHI, and flavonone 3-hydroxylase (Pelletier et al., 1999). The flavonoids accumulate in a tissue-specific pattern that corresponds to areas of auxin accumulation (Ulmasov et al., 1997; Sabatini et al., 1999) and *PIN* gene expression (Galweiler et al., 1998; Muller et al., 1998; Friml et al., 2000). The areas of flavonoid accu-

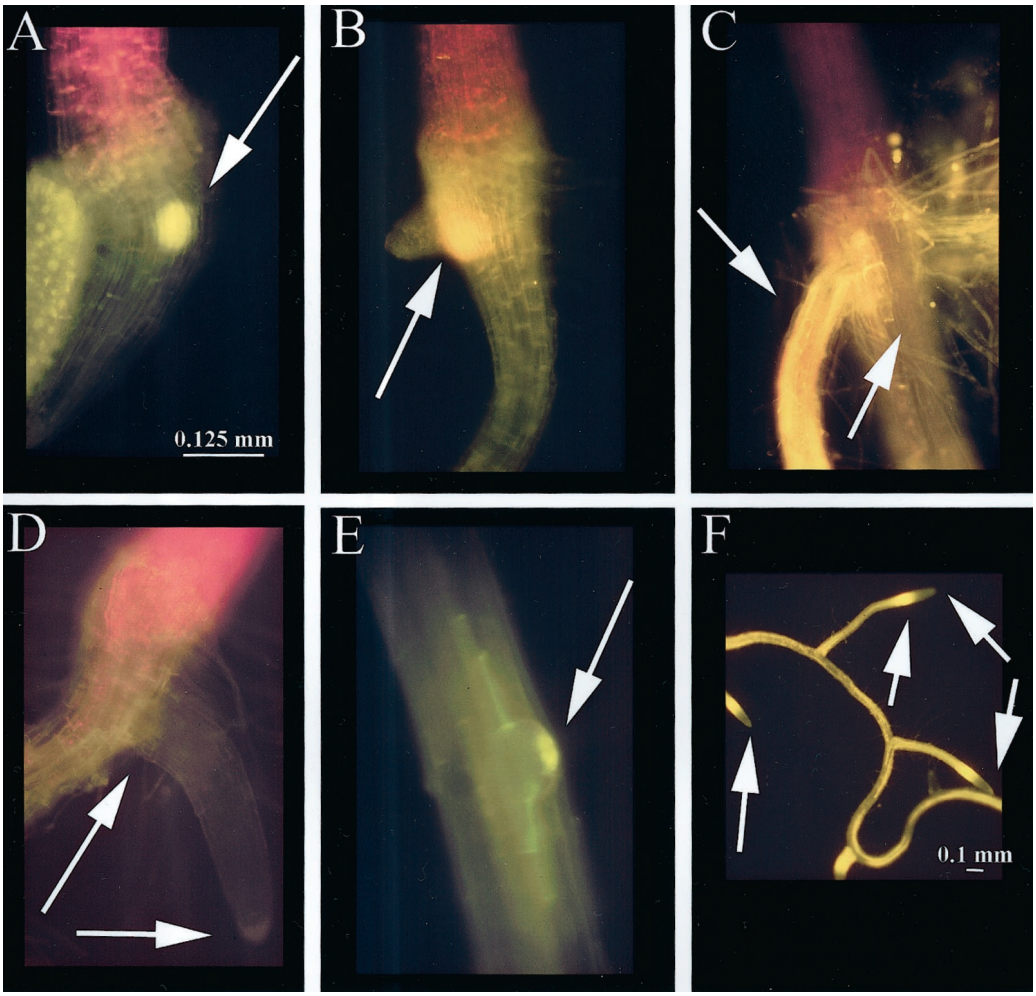

Figure 6. Flavonoid localization during secondary root development viewed through FITC filter. Size bars are 0.125 mm for A through E and 0.1 mm for F. A, *tt3* 7-d secondary root primordium with NC accumulation (arrow). B, *tt3* 7-d-older secondary root primordium with quercetin accumulation (arrow). C, Ler 8-d mature secondary roots with quercetin accumulation. Arrows point to quercetin in adventitious root and to non-staining primary root. D, *tt4*(85) 7-d abnormal placement of secondary root, no pigment accumulation observed. E, *tt7* 6-d secondary root primordium with kaempferol at root tip (arrow). F, Ler 7- to 8-d secondary roots occurring midpoint on the primary root resembles root tip of primary root. Arrows point to distal elongation zone and root cap.

mulation also define TZ between different organs, including the cotyledonary node transition, root-shoot transition, and transition from the meristematic to elongation zones in roots. The role of this accumulation may be to modulate auxin flow between these different organs. The cotyledonary node TZ between the UH and the epicotyl is based on the vascular tissue differences at the node and that of the subtending hypocotyl (Busse and Evert, 1999). The hypocotyl/root TZ is generally the lower boundary of chloroplast formation and is the uppermost region where suberized Casparian strips form in the root endodermis (A. Murphy, unpublished data). A single ring of epidermal cells at this boundary also produces a profusion of epidermal root hairs. In roots, the distal elongation zone is a TZ between the meristematic region and the central elongation zone, and in Arabidopsis begins about 100 microns from the root tip (Mullen et al., 1998), which is the region of intense flavonoid staining in the root tip. In adult plants, flavonoid accumulation is restricted to actively growing or maturing tissue.

Accumulation of flavonoid derivatives is also developmentally regulated. Our HPLC/MS/spectroscopic analysis of whole and sectioned seedlings confirmed earlier reports (Sheahan and Cheong, 1998; Pelletier et al., 1999) that glycosylated flavonoids comprise a large proportion of the total flavonoids as early as 5 d, but also indicated that they are limited to the cotyledons and the UH until 7 d. Aglycone forms predominate in the hypocotyl/root TZ and root tip, and it is not until 7 d that the majority of flavonoids are glycosylated in all sections. This biochemical analysis corresponds to the in situ DPBA staining patterns of whole seedlings. Since the aglycone forms are hydrophobic and associated with membranes,

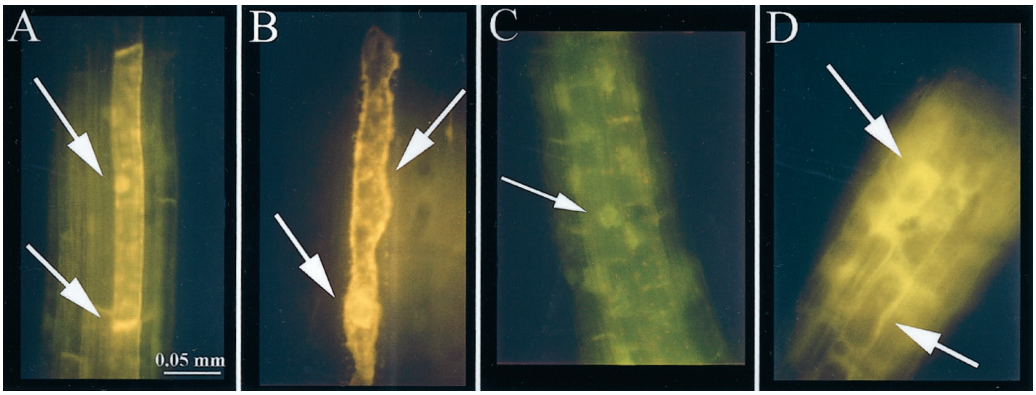

Figure 7. Subcellular flavonoid localization in plasmolyzed roots of 6-d *tt* seedlings. Plasmolysis time indicated viewed through FITC filter. Size bar is 0.05 mm for A through D. A, *tt3* after 2 min. Quercetin localized to basal end of plasma membrane in cells (arrow). B, *tt3* after 5 min. Quercetin localized to plasma membrane and other internal membranes (arrows). C, *tt7* after 2 min. Kaempferol localized to nucleus (arrow). D, *tt5* after 2 min. NC localized diffusely throughout the cytosol (arrows).

their localization in the TZ is consistent with their role in regulating auxin efflux. Both the flavonoid species present and its localization are important in regulation of auxin distribution.

Flavonoid Accumulation in *tt* Mutants

Flavonoid profiles in the mutants are generally altered according to predictions based on the biochemical pathway, with one exception that indicates that one reaction may be more complex than expected. Naringenin is the intermediate expected to accumulate in *tt6*, but was not detected by any of the methods used here. This result may be explained by a report from Sheahan et al. (1998) that an unidentified orthodihydroxy or orthotrihydroxy flavonoid is, in fact, the predominant flavonoid accumulating in *tt6*. This suggests that naringenin is unstable or is quickly converted into another compound. As the flavonoid biosynthetic pathway is under feedback control (Pelletier et al., 1999), and naringenin itself regulates transcription of genes encoding its biosynthetic enzymes (Pelletier et al., 1999). The accumulation of other flavonoid compounds in *tt5* and *tt7* may be the result of altered feedback mechanisms in the mutants and the compounds' subsequent availability to other enzymes.

Developmental differences were noted in the *tt* mutants compared with wild type, and differences in *tt4* are discussed in the companion paper by Brown and coworkers (2001). It is now possible to begin to investigate the underlying causes of these developmental defects.

Localization

The intermediates and final products of the flavonoid pathway accumulate in the same cells and tissues in the *tt* mutants and wild type, respectively. This result supports the hypothesis that flavonoids are synthesized in the same cells in which they accumulate. Quercetin localization in the plasma membrane at the basal ends of cells is consistent with the basally located AtPIN1 (Galweiler et al., 1998) and NPA-binding protein that Jacobs and Gilbert (1983) described, lending further support that flavonoids are endogenous regulators of auxin transport (Jacobs and Rubery, 1988; Murphy et al., 2000; Brown et al., 2001). Nuclear localization of kaempferol and quercetin, perhaps as derivatives, suggests that they may function as antioxidants or transcriptional regulatory factors, as sulfonated forms of flavonoids have been identified in the nucleus (Grandmaison and Ibrahim, 1996). The subcellular localization of these flavonoids in Arabidopsis is consistent with the membrane association of the enzyme complexes of the flavonoid pathway (Shirley, 1999) and with previous studies (Sheahan and Cheong, 1998; Hutangura et al., 1999).

Flavonoids and NPA Amidase/Aminopeptidase (AP) Activity Colocalize

The regions of flavonoid staining in Arabidopsis—cotyledonary node, hypocotyl-root TZ, distal elongation zone and root cap, and bases of root primordia along the vascular tissue, stigmata, flowers, and primordia—are identical to the regions stained in histochemical assays of NPA amidase activity, and Tyr-, Trp-, and Pro-AP activity (Murphy and Taiz, 1999a, 1999b). This, along with the observations that Tyr-, Trp-, and Pro-β-naphthylamide conjugates have NPA-like activity, and that flavonoids inhibit NPA-binding and AP activity, suggests a role for flavonoids and APs in stimulating auxin retention in plant tissues (Murphy et al., 2000). However, biochemical evidence suggests that aglycone flavonoids do not directly bind the catalytic site of the plasma membrane APs (Murphy et al., 2000) and, therefore, modulate AP activity indirectly.

CONCLUSIONS

There is increasing evidence that auxin retention, i.e. the inhibition of auxin transport, is as important as auxin transport itself in determining the steady-state distribution of auxin in the plant. Localized regions of auxin retention can lead to auxin accumulation, which, in turn, may trigger developmental events. Flavonoids have long been suspected to be positive regulators of auxin retention despite being less effective at inhibiting auxin transport than artificial inhibitors such as NPA (Jacobs and Rubery, 1988; Faulkner and Rubery, 1992). Membrane-bound aglycone flavonoids specifically colocalize with regions of auxin accumulation in Arabidopsis seedlings and mature plants. Since flavonoid precursors also colocalize to these regions, it appears that they act in the same cells in which they are synthesized. This flavonoid localization suggests that aglycone flavonoids function as autocrine effectors that have a role in auxin distribution.

MATERIALS AND METHODS

Reagents and Seed Stocks

All chemicals were from Sigma (St. Louis). Col-0, Ler, *tt3-1*(84), *tt4*(85), *tt5-1*(86), *tt6-1*(87), and *tt7-1*(88)] seeds in the Ler background, and *fah1-2* seeds were obtained from the Arabidopsis Biological Resource Center at Ohio State University, and the null mutant seeds *tt4* (2YY6) and *tt4* (UV118a) were generous gifts from Brenda Winkle-Shirley (Saslowsky et al., 2000). Yellow seeds of *tt4(85)* were selected for two generations prior to analyses of flavonoids and growth characteristics.

Growing Conditions and Flavonoid Staining in Seedlings

Five hundred seedlings of each type were grown and stained as previously described (Sheahan and Rechnitz, 1993; Murphy et al., 2000) with tissue-specific modifications. Seedlings were stained for 5 to 15 min using saturated (0.25%, w/v) DPBA with 0.005% (v/v, seedling photographs) or 0.02% (v/v, plasmolysis photographs) Triton X-100 and were visualized with an epifluorescent microscope equipped with an FITC filter (excitation 450–490 nm, suppression LP 515 nm). Where indicated, seedlings were plasmolyzed with 2 M mannitol for 2 or 5 min prior to staining. Photodocumentation of seedlings was achieved with color slide film (Kodak Elite, ASA 400, Kodak, Rochester, NY) after 5 min of staining. Flavonoid fluorescence of stained seedlings visually increased up to 15 min, then quenching was observed.

Growing Conditions and Flavonoid Staining in Mature Ler Plants

Adult plants were grown in a growth chamber with 10 h of white light (100 μmol m^{-2} s^{-1}; mixed fluorescent and incandescent bulbs) with a day temperature of 21°C and 14 h of darkness with a night temperature 18°C. Adult tissues were stained for 15 min (flowers) or 2 h (whole plants) with 0.25% (w/v) DPBA and 0.1% (v/v) Triton X-100 (Sheahan and Rechnitz, 1992). The fluorescence in whole adult plants was visualized with a UV light source (305 nm peak emission); the fluorescence of flowers were viewed with an epifluorescence microscope.

Growing Conditions and Flavonoid Staining in Mature Col-0 Plants

For staining of inflorescence stems, a 0.005% (w/v) solution of norflurazon (2.4% [v/v] ethanol) with 0.01% (v/v) Triton X-100 was applied to the apical meristem just prior to initiation of floral meristems (d 26 of growth). Within days, bleached inflorescence stems arise from green rosettes; however, these inflorescence stems do not grow to the same height as inflorescence stems of untreated plants. To detect flavonol distribution throughout the intact inflorescence, the entire plant was gently removed from the soil and was placed into the staining solution described above. Fluorescence was viewed using a hand-held UV light or the UV filter set of the microscope.

Confirmation of Flavonoid Identity and Identification of Flavonoid Content in Seedling Sections

Fluorescence of flavonoid standards in complex with DPBA were visualized with a UV light source (305 nm maxima). Fluorescence maxima of flavonoid standards within the FITC filter range were determined fluorometrically and were obtained for the following standards: naringenin (515, 522sh, 523sh, and 527 nm), phloretin (518, 520, and 523 nm), apigenin (516 nm), taxifolin (dihydroquercetin; 517 and 522 nm), kaempferol (520 nm), quercetin (543 nm), and quercitrin (534 nm); flavonols and dihyroflavonols fluorescence 10- to 100-fold more than other flavonoids. Flavonoid localization was confirmed microscopically by visualization after treatment with NH_3 vapor for 2 min or with 5% (w/v) $AlCl_3$ in 95% (v/v) ethanol for 10 min.

For HPLC analysis approximately 500 5-d seedlings of each line were excised into the following sections: UH, LH, TZ/UR, and LR. The sections were collected, blotted dry briefly, and weighed in a tared Eppendorf tube. Seedlings sections were extracted in 90% (v/v) methanol (10 μL mg fresh $weight^{-1}$) as described by Burbulis et al. (1996) and were then analyzed by TLC ($\pm NH_3$), UV/vis spectrophotometry (Harborne et al., 1975; Markham, 1982), and HPLC. Identities of HPLC UV absorbance peaks were compared with the elution profiles and fluorescence spectra of genuine standards and were confirmed by UV/vis spectrophotometric shift analysis according to the method of Markham (1982). In cases where positive identification could not be made, molecular mass determination was by electrospray + MS, as described previously (Murphy and Taiz, 1999a). Identities of HPLC peaks were further con-

firmed by comparison with profiles published by Graham (1991), Burbulis et al. (1996), Sheahan et al. (1998), and Pelletier et al. (1999).

Flavonoid glycosides and aglycones were prepared for analysis from seedling sections as described by Burbulis et al. (1996) and were analyzed by HPLC using a C18 column (4.2 × 250 mm, 5 μm, Supelco, Bellefonte, PA) with a CC 410 pump (Perkin Elmer, Norwalk, CT) with UV absorbance monitoring at 254 nm with a UV/vis absorbance monitor (Spectraflow 773, Kratos, Ramsey, NJ) and fluorescence monitoring with excitation at 367 nm and emission at 515, 520, 527, 534, or 543 nm (Waters 870, Waters, Bedford, MA) to confirm identities of individual peaks. Separation was achieved with a gradient of 2% (v/v) methanol in water (pH 3.0 with H_3PO_4) and acetonitrile at a flow rate of 1 mL min^{-1} with a highly concave profile (16 min for unhydrolyzed flavonoids and 30 min for aglycone products of acid hydrolysis). The values were integrated and normalized to the injection of naringenin standard (20 μL of 10 ng μL^{-1} in MeOH). Results shown do not include quantitation of peaks identified spectrophotometrically as sinapate esters, although sinapate contents of seedlings were consistent with those found in the literature (Sheahan, 1996; Ruegger et al., 1999). Peaks were also analyzed spectrofluorimetrically, and matched previously reported data (Chapple et al., 1992; Sheahan, 1996; Sheahan and Cheong, 1998). Peaks were collected and analyzed spectrophotometrically according to Markham (1982) and Harborne et al. (1975). Molecular weights of flavonoid skeletons of individual peaks were identified by electrospray + MS, as previously described (Murphy et al., 1999a).

Flavonoid and Anthocyanin Content of Inflorescence Stems

Inflorescence stems were divided into 2-mm sections. Flavonoids were extracted and analyzed by HPLC as above. Anthocyanins were extracted and analyzed by spectrophotometry (Adamse et al., 1989).

ACKNOWLEDGMENTS

We thank Brenda Winkle-Shirley for her generous gift of the *tt4* (UV118a) null mutant seeds, Dior Kelly for the light intensity data, Jonathon Krupp for assistance with the microscopy, and Debra Sherman for assistance with color printing.

Received February 14, 2001; returned for revision February 21, 2001; accepted March 22, 2001.

LITERATURE CITED

Adamse P, Peters JL, Jaspers PAPM, van Tuinen A, Koornneef M, Kendrick RE (1989) Photocontrol of anthocyanin synthesis in tomato seedlings: a genetic approach. Photochem Photobiol **50:** 107–111

Bernasconi P (1996) Effect of synthetic and natural protein tyrosine kinase inhibitors on auxin efflux in zucchini (*Cucurbita pepo*) hypocotyls. Physiol Plant **96:** 205–510

Brown DE, Rashotte AM, Murphy AS, Tague BW, Peer WA, Taiz L, Muday GK (2001) Flavonoids act as negative regulators of auxin transport in vivo in *Arabidopsis thaliana.* Plant Physiol **126:** 524–535

Burbulis IE, Iacobucci M, Shirley BW (1996) A null mutation in the first enzyme of flavonoid biosynthesis does not affect male fertility in *Arabidopsis.* Plant Cell **8:** 1013–1025

Busse JS, Evert RF (1999) Vascular differentiation and transition in the seedling of *Arabidopsis thaliana* (Brassicaceae). Int J Plant Sci **160:** 241–251

Chapple C, Vogt T, Ellis BE, Somerville CR (1992) An *Arabiodopsis* mutant defective in the general phenylpropanoid pathway. Plant Cell **4:** 1413–1424

Debeaujon I, Leon-Kloosterziel KM, Koornneef M (2000) Influence of the testa on seed dormancy, germination, and longevity in Arabidopsis. Plant Physiol **122:** 403–413

Faulkner IJ, Rubery PH (1992) Flavonoids and flavonoid sulphates as probes of auxin-transport regulation in *Cucurbita pepo* hypocotyl segments and vesicles. Planta **186:** 618–625

Friml J, Wisniewska J, Benkova E, Hamman T, Nettesheim K, Tanzler P, Palme K (2000) Molecular characterization of new members of the *Arabidopsis PIN* gene family (abstract no. 212). Presented at the 11th Annual International Conference on Arabidopsis Research, June 24–28, 2000, Madison, WI

Galweiler L, Guan C, Muller A, Wisman E, Mendgen K, Yephremov A, Palme K (1998) Regulation of polar auxin transport by AtPIN1 in *Arabidopsis* vascular tissue. Science **282:** 2226–2230

Graham T (1991) A rapid, high resolution high performance liquid chromatography profiling procedure for plant and microbial aromatic secondary metabolites. Plant Physiol **95:** 584–593

Graham T (1998) Flavonoid and flavonol glycoside metabolism in *Arabidopsis*. Plant Physiol Biochem **36:** 165–144

Grandmaison J, Ibrahim RK (1996) Evidence for nuclear protein binding of flavonol sulfate esters in *Flaveria chloraefolia*. J Plant Physiol **147:** 653–660

Harborne JB, Mabry T, Mabry H (1975) The Flavonoids. Chapman and Hall, London

Hutangura P, Mathesius U, Jones MGK, Rolfe B (1999) Auxin induction is a trigger for root gall formation caused by root-knot nematodes in white clover and is associated with the activation of the flavonoid pathway. Aust J Plant Physiol **26:** 221–231

Jacobs M, Gilbert SF (1983) Basal localization of the presumptive auxin transport carrier in pea stem cells. Science **220:** 1297–1300

Jacobs M, Rubery PH (1988) Naturally occurring auxin transport regulators. Science **241:** 346–349

Koornneef M (1990) Mutations affecting the testa color in *Arabidopsis.* Arabidopsis Inf Serv **28:** 1–4

Koornneef M, Luiten W, de Vlaming P, Schram AW (1982) A gene controlling flavonoid-3′-hydroxylation in *Arabidopsis.* Arabidopsis Inf Serv **19:** 113–115

Marigo G, Boudet AM (1977) Relations polyphénols croissance: mise en èvidence d'un effect inhibiteur des com-

posés phénoliques sur le transport polarisé de l'auxine. Physiol Plant **41:** 197–202

Markham KR (1982) Techniques of Flavonoid Identification. Academic Press, London

Mathesius U, Bayliss C, Weinman JJ, Schlaman HRM, Spaink HP, Rolfe BG, McCully ME, Djordjevic MA (1998a) Flavonoids synthesized in cortical cells during nodule initiation are early developmental markers in white clover. Mol Plant-Microbe Interact **11:** 1223–1232

Mathesius U, Schlaman HRM, Spaink HP, Sautter C, Rolfe BG, Djordjevic MA (1998b) Auxin transport inhibition precedes root nodule formation in white clover roots and is regulated by flavonoids and derivatives of chitin oligosaccharides. Plant J **14:** 23–34

Mullen JL, Ishikawa H, Evans ML (1998) Analysis of the changes in relative elemental growth rate patterns in the elongation zone of *Arabidopsis* roots upon gravitropism. Planta **206:** 598–603

Muller A, Guan C, Galweiler L, Tanzler P, Huijser P, Marchant A, Parry G, Bennett M, Wisman E, Palme K (1998) AtPIN2 defines a locus of *Arabidopsis* for root gravitropism control. EMBO J **17:** 6903–6911

Murphy A, Peer WA, Taiz L (2000) Regulation of auxin transport by aminopeptidases and endogenous flavonoids. Planta **211:** 315–324

Murphy A, Taiz L (1999a) Naphthylphthalmic acid is enzymatically hydrolyzed at the hypocotyl-root transition zone and other tissues in *Arabidopsis thaliana* seedlings. Plant Physiol Biochem **37:** 413–430

Murphy A, Taiz L (1999b) Localization and characterization of soluble plasma membrane aminopeptidase activities in *Arabidopsis* seedlings. Plant Physiol Biochem **37:** 431–443

Pelletier MK, Burbulis IE, Winkel-Shirley B (1999) Disruption of specific flavonoid genes enhances the accumulation of flavonoid enzymes and end-products in *Arabidopsis* seedlings. Plant Mol Biol **40:** 45–54

Ruegger M, Meyer K, Cusumano JC, Chapple C (1999) Regulation of ferulate-5-hydroxylase expression in *Arabidopsis* in the context of sinapate ester biosynthesis. Plant Physiol **119:** 101–110

Sabatini S, Beis D, Wolkenfelt H, Murfett J, Guilfoyle T, Malamy J, Benfey P, Leyser O, Bechtold N, Weisbeek P, Scheres B (1999) An auxin-dependent distal organizer of pattern and polarity in the *Arabidopsis* root. Cell **99:** 463–472

Saslowsky DE, Dana CD, Winkle-Shirley B (2000) An allelic series for the chalcone synthase locus in *Arabidopsis*. Gene **255:** 127–138

Sheahan JJ (1996) Sinapate esters provide greater UV-B attenuation than flavonoids in *Arabidopsis thaliana* (Brassicaceae). Am J Bot **83:** 679–686

Sheahan JJ, Cheong H (1998) The colorless flavonoids of *Arabidopsis thaliana* (Brassicaceae): II. Flavonoid 3′ hydroxylation and lipid peroxidation. Am J Bot **85:** 476–480

Sheahan JJ, Cheong H, Rechnitz GA (1998) The colorless flavonoids of *Arabidopsis thaliana* (Brassicaceae): I. A model system to study the orthodihydroxy structure. Am J Bot **85:** 467–475

Sheahan JJ, Rechnitz GA (1992) Flavonoid-specific staining of *Arabidopsis thaliana*. Biotechniques **13:** 880–883

Sheahan JJ, Rechnitz GA (1993) Differential visualization of transparent testa mutants in *Arabidopsis thaliana*. Anal Chem **65:** 961–963

Shirley BW (1999) Evidence for enzyme complexes in the phenylpropanoid and flavonoid pathways. Physiol Plant **107:** 142–149

Shirley BW, Kubasek WL, Storz G, Bruggeman E, Koornneef M, Ausubel FM, Goodman HM (1995) Analysis of *Arabidopsis* mutants deficient in flavonoid biosynthesis. Plant J **8:** 659–671

Stafford H (1990) Flavonoid Metabolism. CRC Press, Boca Raton, FL

Stenlid G (1976) The effects of flavonoids on polar auxin transport. Physiol Plant **38:** 262–266

Ulmasov T, Murfett J, Hagen G, Guilfoyle TJ (1997) Aux/IAA proteins repress expression of reporter genes containing natural and highly active synthetic auxin response elements. Plant Cell **9:** 1963–1971

Wisman E, Hartmann U, Sagasser M, Baumann E, Palme K, Hahlbrock K, Saedler H, Weissar B (1998) Knock-out mutants from *En-1* mutagenized *Arabidopsis thaliana* population generate phenylpropanoid biosynthesis phenotypes. Proc Natl Acad Sci USA **95:** 12432–12437